Atmospheric Research 208 (2018) 60–77

Contents lists available at ScienceDirect

Atmospheric Research

journal homepage: www.elsevier.com/locate/atmosres

Statistical analyses of extreme rainfall events in Thessaloniki, Greece

Maria Douka*, Theodore Karacostas

Department of Meteorology and Climatology, School of Geology, Aristotle University of Thessaloniki, Thessaloniki, Greece

ARTICLE INFO

Keywords:
Extreme precipitation
Hourly rainfall measurements
Hourly threshold precipitation
Probability distributions
Goodness-of-fit test
Return period

ABSTRACT

Concern about climate change has amplified the need for accurate information about variations in statistical characteristics of extreme rainfall events in both smaller temporal and spatial scale. For this reason, in this paper the hourly precipitation measurements obtained at the Department of Meteorology and Climatology of the Aristotle University of Thessaloniki meteorological station, during the period 1947–2003, are used. A new threshold determining method is proposed, in order to define the extreme rainfall event in Thessaloniki, based upon the polynomial trends of the cumulative distribution functions, retrieved from hourly precipitation measurements. Through this approach, three statistical goodness-of-fit tests were carried out, in order to come up with the best fitting probability distributions, for annual and seasonal extreme precipitation conditions. Based upon this fitting distribution procedure, return periods for different precipitation extreme values were calculated. Results indicate that the value of 6.5 mm/h is the hourly threshold of extreme precipitation in Thessaloniki over the studied period. Furthermore, the Generalized Pareto, and the Johnson SB, the log-Gamma and the Lognormal are the best fitted probability models for the description of annual and seasonal extreme rainfall events, respectively. Last but not least, the contribution of hourly data in the accuracy of the results is discussed.

1. Introduction

According to the IPCC reports (2007), the global warming, that is derived from the positive concentrations of greenhouse gases, has a possible influence on the global hydrological cycle. Characteristically, Trenberth (1999) observed that the increased ultraviolet radiation that is produced by the greenhouse effect, contributes on a further increase of evaporation. This results in the strengthening of the atmosphere's capacity to hold water vapor in hot days, which in its turn causes intensification of the hydrological cycle and increase of the frequency of extreme rainfall events. Therefore, changes that will potentially happen in the distribution of extreme precipitation are crucial and of a great research interest, due to its enormous impact on humans, their properties, and the environment.

A lot of scientific work has already been done worldwide on the subjects related to the probability distributions of extreme precipitation. As it is expected, the outcomes vary according to the objective, methodology, study area and database of each study. For example, Zalina et al. (2002) reported that the Generalized Extreme Value (GEV) shows very good descriptive and predictive abilities of the annual extreme rainfall series in Peninsular Malaysia, while Koutsoyiannis (2004) concluded that neither of the two-parameter special cases of the GEV distribution (Gumbel and Frechet ones) is appropriate for modeling the annual maximum rainfall series in Europe and USA. Analogous studies have been performed at several single sites all over the world (Hirose, 1994; Nadarajah and Withers, 2001; Chu et al., 2009), as the geographical characteristics of the studied area affect substantially the spatial variability of extreme precipitation events. These studies play a significant role in the prevention of the flood damage caused by extreme rainfall events, since they are considered to be invaluable tools for the construction of certain projects, such as drainage systems and dams.

Although bibliography seems to be extensive on the studies of extreme precipitation (Bocheva et al., 2009; Müller et al., 2009; Xu et al., 2011; Fernández-Montes et al., 2014; Santos and Fragoso, 2013; Song et al., 2015; Gao et al., 2016), very few researchers examined the statistical analyses of extreme rainfall conditions by using hourly precipitation measurements (Winkler, 1992; Kanae et al., 2004; Fujibe et al., 2005; Sen, 2008; Twardosz, 2010; Lenderink et al., 2011). This could be attributed to the rarity of these data. However, the validity of the results of the statistical analyses could be improved through the study of the extreme rainfall events in a smaller temporal scale than daily. The utilization of hourly records is more beneficial, as the heavy precipitation events occurring mainly in the warm period of the year, are characterized by their short duration. In Greece, the studies using hourly precipitation measurements are limited. Particularly, in Thessaloniki the investigation of the diurnal rainfall pattern is the unique example of using hourly rainfall data and was carried out by Giles and

* Corresponding author.
E-mail address: maridouk@geo.auth.gr (M. Douka).

http://dx.doi.org/10.1016/j.atmosres.2017.08.025
Received 31 May 2017; Received in revised form 11 August 2017; Accepted 29 August 2017
Available online 28 September 2017
0169-8095/ © 2017 Elsevier B.V. All rights reserved.

Flocas (1990).

As far as the definition of extreme precipitation is concerned, both parametric and non-parametric statistical techniques are usually adopted, in order to identify the rainfall threshold above which a precipitation event can be characterized as an extreme one. Feng et al. (2007) were the first researchers who have applied the Block Maxima method for the modeling of annual extreme rainfall in China. In addition, the Peak over Threshold method was proposed by Anagnostopoulou and Tolika (2010 and 2012), as the best parametric approach for the fitting of a statistical distribution to the tails of an unknown distribution. On the other hand, the absolute threshold of 60 mm/day was used by Karagiannidis et al. (2012), in order to investigate the climatological aspects of extreme precipitation related to mid-latitude cyclonic systems in Europe. In a similar approach to the problem, Bocheva et al. (2010) adopted the threshold of 100 mm/day for the climatic analysis of the torrential precipitation in Bulgaria. In the present study, the selection of a fixed absolute threshold is deemed to be the most appropriate and efficient technique, as it could contribute significantly to the understanding of the impact of extreme rainfalls on society in local scales.

The purpose of this study is to define the most representative absolute hourly threshold of extreme precipitation events in Thessaloniki. The determination was succeeded through a new proposed method based on the coefficients of the independent variables of the polynomial regression lines of the cumulative probability distributions of some data sets, created from hourly rainfall records. Utilizing the hourly precipitation measurements of the meteorological station of the Department of Meteorology and Climatology of the Aristotle University of Thessaloniki, covering a 57-year period, the best fitted probability distributions were identified on both, annual and seasonal scale, as well as, the return levels of some of the most extreme rainfall events were calculated.

In Section 2, a detailed description of both the materials and the methodology used, is provided. The analyses of the results for the determination of the fixed hourly threshold of extreme rainfall in Thessaloniki is provided in Section 3. Moreover, the outcomes of the best fitted distributions of extreme precipitation in the studied area are discussed in this section. The conclusions are drawn in Section 4.

2. Materials and methodology

2.1. Study area and data

Thessaloniki (40° 37′ N, 22° 95′ E) is the capital of the region of Macedonia in Northern Greece, as well as, the second largest city in the country (Fig. 1a). The city is situated at the heart of Thermaikos gulf in the Northern Aegean Sea. The climate of the area is a typical Mediterranean mild climate with bimodal seasonal variation of precipitation. According to Köppen classification, it is characterized as Csa. The principal maximum and minimum are observed in December and August, respectively. The mean annual precipitation and its standard deviation is: 451.7 mm ± 96.3 mm, according to Stathis and Mavromatis (2009), for the period 1930–2004 and 475.6 mm ± 105.4 mm, according to Pakalidou and Karacosta (2016), for the much longer period of 1892–2015.

The data used in this study are the only available hourly measurements of precipitation obtained at the Meteorological Station of the Department of Meteorology and Climatology of the Aristotle University of Thessaloniki (AUTH) for the period 1947–2003. Stathis and Mavromatis (2009), by applying the Bartlett's test of homogeneity, examined the homogeneity of precipitation measurements at Thessaloniki, for a little longer period (1930–2004), using monthly, seasonal and annual precipitation measurements. The results suggest that AUTH has exhibited great precipitation homogeneity, which could be attributed to the unchanged position since 1930. As far as the investigation of the randomness of the examined time series of precipitation is concerned, they concluded that non-randomness is present in the data in accordance with the Cramer's test.

2.2. The definition of the hourly threshold of extreme rainfall in Thessaloniki

According to the Glossary of Meteorology (Huschke, 1959), precipitation is characterized as heavy, when its intensity exceeds 7.62 mm/h. Based upon this indication, a set of ten (10) candidate thresholds {*3.5 mm/h, 4.0 mm/h, 4.5 mm/h, 5.0 mm/h, 5.5 mm/h, 6.0 mm/h, 6.5 mm/h, 7.0 mm/h, 7.5 mm/h, 8.0 mm/h*} was adopted, aiming at the selection of the most proper and representative hourly threshold of extreme precipitation events in Thessaloniki, during the studied period.

Taking into consideration the aforementioned set of data, *the daily rainfall for each candidate threshold is defined as the highest hourly value that exceeds the i-candidate threshold over a 24-h period, where* $i = 1, \ldots, 10$. The daily rainfall of the days with hourly measurement less than the i-candidate threshold is considered to be 0. As a consequence, ten (10) sets of data information were constructed (one for each candidate threshold), which contain the daily rainfall values of the period 1947–2003. Having explained what is meant by daily rainfall values in the particular study, *the daily extreme rainfall values are defined as the no zero daily rainfall ones for each set of information*. The reconstructed sets of data information, which now contain the daily extreme rainfall values of the studied period, were fully described by the best-fitted extreme value theoretical distributions according to Kolmogorov-Smirnov goodness-of-fit test.

In the following two sub-sessions of this paragraph, the procedure followed for the definition of the hourly threshold of extreme rainfall in the studied area over the period 1947–2003 was described visually and deterministically. Moreover, a schematic overview of the aforementioned procedure is demonstrated in Fig. 1b

2.2.1. Visual definition of the hourly threshold of extreme rainfall in Thessaloniki

The visual identification of the hourly threshold of extreme precipitation in Thessaloniki was achieved by the illustration of the aforementioned ten (10) cumulative distributions in a figure. The use of the cumulative distributions for each candidate set is attributed to the fact that they are better comparable than the probability density functions according to Reimann et al. (2005), and from the theoretical point of view, the cumulative distributions usually provide a more comprehensive and thorough picture of the function itself. In addition, the slope of the cumulative distribution of “extreme hourly rainfall” of Thessaloniki should tend to differ from the other ones. Specifically, a potential sudden change in the slope between the successive cumulative curves indicates the most appropriate hourly threshold of extreme rainfall over the studied period.

2.2.2. Deterministic definition of the hourly threshold of extreme rainfall in Thessaloniki

In order to increase the reliability of the hourly threshold that was selected with the visual method in Section 2.2.1, the use of a more objective procedure is deemed necessary. The key-steps can be listed as follows:

a) Firstly, the 3rd order polynomial trendlines of the cumulative distributions for each candidate threshold were calculated, as the coefficients of their independent variables are able to define

(a)

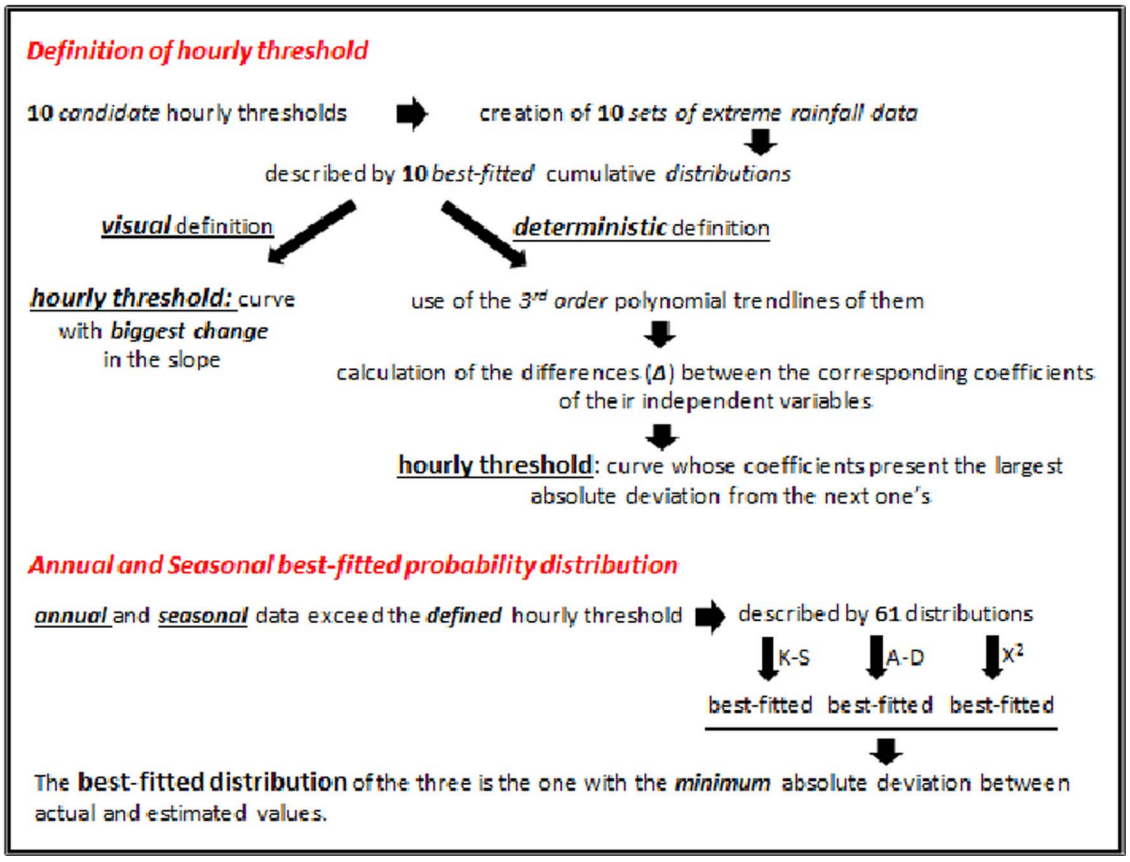
Definition of hourly threshold
10 candidate hourly thresholds
creation of 10 sets of extreme rainfall data
described by 10 best-fitted cumulative distributions
visual definition
deterministic definition
hourly threshold: curve with biggest change in the slope
use of the 3rd order polynomial trendlines of them
calculation of the differences (Δ) between the corresponding coefficients of their independent variables
hourly threshold: curve whose coefficients present the largest absolute deviation from the next one's
Annual and Seasonal best-fitted probability distribution
annual and seasonal data exceed the defined hourly threshold
described by 61 distributions
K-S
A-D
X²
best-fitted
best-fitted
best-fitted
The best-fitted distribution of the three is the one with the minimum absolute deviation between actual and estimated values.

(b)

Fig. 1. (a). Topography of Northern Greece.
(b). Schematic overview of the adopted and followed up methodology, for the definition of the hourly threshold and for the identification of the best-fitted distribution, annually and seasonally.

numerically their slope.

b) To determine the sudden change in the slope of the successive cumulative distributions of the ten (10) data sets, the differences (Δ) between the corresponding coefficients of their independent variables were calculated as follows:

$$\boldsymbol{\Delta} = |\boldsymbol{\alpha}_{(i+1)j} - \boldsymbol{\alpha}_{ij}| \quad i = 1...9 \; and \; j = 1, 2, 3 \tag{1}$$

where α_{ij} and $\alpha_{(i+1)j}$ are the coefficients of the independent variables of the regression line of the cumulative distribution for each candidate hourly threshold and, for each next one, respectively.

c) Lastly, the curve whose coefficients present the largest absolute deviation from the corresponding coefficients of the next one, indicate the hourly threshold of extreme precipitation in Thessaloniki over the examined period 1947–2003.

2.3. Fitting the probability distributions to the data

The climate prevailing during the twelve (12) months in Thessaloniki is characterized by four (4) seasons, that is: winter (December – February), spring (March – May), summer (June – August) and autumn (September – November). Hence, the data exceeding the threshold selected in the present study with the method presented in Section 2.2 were classified in annual and seasonal basis. A set of 61 probability distributions were then employed for the evaluation of the best fitted probability model for extreme precipitation for each period. In particular, the following statistical distributions were applied: Beta, Burr (3P and 4P), Cauchy, Chi-Squared (1P and 2P), Dagum (3P and 4P), Erlang (2P and 3P), Error, Error Function, Exponential (1P and 2P), Fatigue Life (2P and 3P), Frechet (2P and 3P), Gamma (2P and 3P), Generalized Extreme Value, Generalized Gamma (3P and 4P), Generalized Pareto, Gumbel Max, Gumbel Min, Hyperbolic Secant, Inverse Gaussian (2P and 3P), Johnson SB, Johnson SU, Kumaraswamy, Laplace, Levy(1P and 2P), Log-Gamma, Log-Logistic (2P and 3P), Log-Pearson 3, Logistic, Lognormal (2P and 3P), Nakagami, Normal, Pareto (1 and 2), Pearson 5 (2P and 3P), Pearson 6 (3P and 4P), Pert, Power Function, Rayleigh (1P and 2P), Reciprocal, Rice, Student's t, Triangular, Uniform, Weibull (2P and 3P). A schematic overview of the adopted and followed up methodology for the identification of the best-fitted distribution is demonstrated in Fig. 1b.

2.4. Testing the-goodness-of-fit and identifying the best fitted probability distribution

The goodness-of-fit tests measure the compatibility of a random sample with a theoretical probability distribution function. In the particular study, three (3) goodness-of-fit tests were employed: the Kolmogorov-Smirnov, the Anderson-Darling and the Chi-Squared tests. One of the most attractive features of Kolmogorov-Smirnov test (Chakravarti et al., 1967) is that it has no restrictions on the sample size comparing to the Chi-Squared goodness-of-fit test (Snedecor and Cochran, 1989), which depends on an adequate one for the approximations to be valid. On the other hand, the Kolmogorov-Smirnov test tends to be more sensitive near the center of the distribution than at the tails. On the contrary, the Anderson-Darling goodness-of-test (Stephens, 1974) which is a modification of the Kolmogorov-Smirnov test, gives more weight to the tails of the distribution.

The aforementioned three (3) goodness-of-fit tests are applied according to the following null hypothesis with the corresponding alternative one:

$\mathbf{H_o}$: *The daily extreme rainfall data follow the specified distribution*.

$\mathbf{H_a}$: *The daily extreme rainfall data does not follow the specified distribution*.

Since the goodness-of-fit test statistics indicate the distance between the data and the fitted distributions, the distribution with the minimum statistic value is the best fitted model for each goodness-of-fit test. Based upon this fact, the sixty-one (61) distributions used in the present study were ranked from 1 (the best fitted one) to 61 (the worst fitted one) and they are fully exhibited in Appendix B. The probability distribution resulted at the first rank was selected for all the three tests, independently. The description of the first rank probability distribution functions, to wit probability density function, range and parameters, is demonstrated in Appendix A. The procedure for obtaining the best fitted probability distribution model, among all the three identified probability distributions that resulted from the three goodness-of-fit tests, is described in the following section. Last but not least, in order to acquire an overview of the results, the quantile plot, the probability plot, as well as the probability density function are taken into consideration.

2.4.1. Generating random numbers

In order to generate random numbers, the parameters of the three best fitted probability distributions that resulted from the three goodness-of-fit tests for each studied period were used, independently. This is succeeded through the Mersenne Twister algorithm (Matsumoto and Nishimura, 1998) that generates a sequence of word vectors, which are w-dimensional row vectors over the two-element field $F_2 = \{0, 1\}$. These word vectors are considered to be uniform pseudorandom integers between 0 and 2w-1. Dividing by 2w-1, each word vector is regarded as a real number in [0, 1]. The algorithm is based upon the following linear recurrence:

$$\boldsymbol{x_{k+n}} := \boldsymbol{x_{k+m}} \oplus (x_k^u \mid \boldsymbol{x'_{k+1}})A, \; \boldsymbol{k} = 0, 1, \ldots \tag{2}$$

where integer n is the degree of the recurrence, integer r (hidden in the definition of $x_k{}^u$) ϵ [0, w-1], integer m ϵ [1, n], and a constant $w \times w$ matrix A with entries in F_2. The Mersenne Twister generator has a period of 2^{19937}–1 ($> 10^{6000}$) and passes numerous tests for its statistical randomness.

2.4.2. Minimum absolute deviation methods

The random numbers generated by the Mersenne Twister algorithm for each one of the three (3) best fitted probability distributions of each studied period were considered as the estimated values of the actual extreme precipitation ones. In order to select the most representative of the three (3) models, the absolute deviation (*AD*) (Mayooran and Laheetharan, 2014) between the actual and estimated extreme precipitation measurements was computed on both annual and seasonal basis, as follows:

$$\boldsymbol{AD} = \left| \sum_{i=1}^{n} (x_i - \hat{x}_i) \right|, \quad (i = 1, 2, \ldots, n) \tag{3}$$

where x_i is the actual extreme precipitation value and $\hat{x}_i$ is the estimated ones. The probability distribution exhibiting the minimum absolute deviation between the actual and estimated values is the most appropriate for the description of annual and seasonal extreme rainfall events in Thessaloniki over the period 1947–2003.

2.5. Return period

Once the best fitted probability distribution model has been identified, the calculation of the return levels, as well as the probability of occurrence of various precipitation extreme values, is of a significant importance and interest.

Return period (T) is the average length of time in years for an event of given magnitude to be equaled or exceeded.

Table 1
The best fitted theoretical distributions to the daily extreme precipitation data sets of the ten (10) candidate thresholds, the statistics, the *P*-values and the critical values for different levels of significance.

Candidate threshold	Theor. distribution	Statistic	P-value	Critical value				
				a = 0.2	**a = 0.1**	a = 0.05	a = 0.02	a = 0.01
3.5 mm/h	Gen.Pareto	0.0364	0.1995	0.0366	0.0417	0.0463	0.0517	0.0555
4.0 mm/h	Gen.Pareto	0.0347	0.3319	0.0396	0.0451	0.0501	0.0560	0.0601
4.5 mm/h	Gen.Pareto	0.0331	0.4905	0.0429	0.0489	0.0543	0.0607	0.0651
5.0 mm/h	Johnson SB	0.0341	0.5543	0.0465	0.0530	0.0589	0.0658	0.0706
5.5 mm/h	Fatigue Life	0.0274	0.8674	0.0498	0.0567	0.0630	0.0704	0.0755
6.0 mm/h	Johnson SB	0.0427	0.4209	0.0525	0.0598	0.0664	0.0743	0.0797
6.5 mm/h	Johnson SB	0.0382	0.6547	0.0566	0.0645	0.0716	0.0800	0.0859
7.0 mm/h	Gen.Pareto	0.0315	0.9116	0.0612	0.0698	0.0775	0.0866	0.0930
7.5 mm/h	Weibull(3P)	0.0389	0.7839	0.0647	0.0738	0.0819	0.0915	0.0982
8.0 mm/h	Gen.Pareto	0.0396	0.8284	0.0690	0.0786	0.0873	0.0976	0.1047

Probability of occurrence (p) is the probability that an event of the specified magnitude will be equaled or exceeded during a one year period.

If n is the total number of values and m is the rank of a value in a descending magnitude ordered list ($x_1 > x_2 > x_3 \ldots > x_m$), the exceeding probability of the m^{th} largest value, x_m, is:

$$\boldsymbol{P}(\boldsymbol{X} \geq x_m) = \frac{m}{n}. \quad (4)$$

A given return level x_T with a return period T may be exceeded once in T years (RamachandraRao and Hamed, 2000). Hence,

$$\boldsymbol{P}(\boldsymbol{X} \geq x_T) = \frac{1}{T}. \quad (5)$$

3. Results and discussion

3.1. The definition of the hourly threshold of extreme rainfall in Thessaloniki

The ten (10) sets of data information, which contain the daily extreme rainfall values of the examined period 1947–2003, were fully described by the best-fitted extreme value theoretical distributions according to Kolmogorov-Smirnov goodness-of-fit test. The theoretical distributions selected as the most appropriate models for the prediction of the daily extreme precipitation in each data set, along with their test statistics, their observed levels of significance (p-value), as well as, their critical values for different levels of significance (a), are provided in Table 1.

It has been noticed that 50% of the sets of data information (the 3.5 mm/h, 4.0 mm/h, 4.5 mm/h, 7.0 mm/h and 8.0 mm/h datasets) are better descripted the Generalized Pareto distribution according to Kolmogorov-Smirnov goodness-of-test, since the values of the test statistics are smaller than the corresponding p-values for all the levels of significance tested. Furthermore, 30% of the candidate datasets (the 5.0 mm/h, 6.0 mm/h and 6.5 mm/h ones) agreed that the Johnson SB is the most representative distribution for the daily extreme rainfall of the studied period. Last but not least, the data exceeds the 5.5 mm/h and 7.5 mm/h candidate thresholds are best represented by the Fatigue Life and the Weibull distributions, with 0.0755 and 0.0982 critical values for a = 0.01, respectively.

The cumulative distributions produced by the aforementioned models for each candidate set of data are illustrated in Fig. 2, aiming at the optical determination of the hourly threshold of extreme rainfall in Thessaloniki.

Considering the displacement of the curves owing to the use of different hourly thresholds, no substantial change in the slope between the successive cumulative distributions was evident. Nevertheless, a more "pronounced" change is observed between the curves of 6.5 mm/h and 7.0 mm/h. This change is better perceptible through the enlargements of the areas 1 and 2. The first area focuses on the part of the graph, where the changes in the slope of the curves occurred, while the area 2 is the subset of area 1 with its most significant change. Concluding, ***the value of 6.5 mm/h is visually defined as the hourly threshold of extreme precipitation in Thessaloniki, during the period 1947–2003***.

The ***deterministic*** definition of the hourly threshold of extreme rainfall in the studied area was succeeded through the use of the 3rd order polynomial trendlines of the cumulative distributions for each candidate threshold, which are exhibited in Fig. 3 with emphasis in the most pronounced differences. It is of crucial importance that the coefficients of the independent variables of the polynomial trendlines are able to define numerically the slope of the curves. The maximum absolute deviation between the corresponding coefficients of the successive curves (Table 3) defines the curve in which the biggest change in the slope is occurred. However, in order to effectively compare the coefficients of independent variables of the successive 3rd order regression lines, it was deemed of significant value to set the beginning of axes as the starting point for all of them.

It is worth mentioning that, in this particular study, the 3rd order polynomial trendlines were preferred to be used, rather than the 2nd and 4th ones. This occurred, because the 3rd regression lines approximate the real data sets fairly well, since their coefficients of determination (R^2) range from 0.855 to 0.916 (Table 2, Fig. 4). On the other hand, the apparent difference of R^2 between the 2nd order polynomial trendlines of the cumulative distributions for the thresholds from 3.5 mm/h to 5.5 mm/h and the 3rd order ones for the corresponding thresholds was the criterion for the rejection of the 2nd order regression line. As far as the 4th order polynomial trendlines are concerned, despite their better fit of the data compared to the 2nd and 3rd order ones, their one more parameter does not contribute significantly to the result. Specifically, the coefficients of determination (R^2) of 4rd order regression lines are approximately 0.9, as well as the corresponding of the 3rd order ones.

The coefficients of the independent variables of the 3rd order polynomial trendlines of the cumulative distributions (α_{ij}), as well as the calculated differences between the successive coefficients (Δ) were demonstrated in Table 3. The absolute deviations were calculated by rounding to the digit of ten millimeters, since the use of more decimal digits was deemed to be unnecessary. As can be seen from the table, the

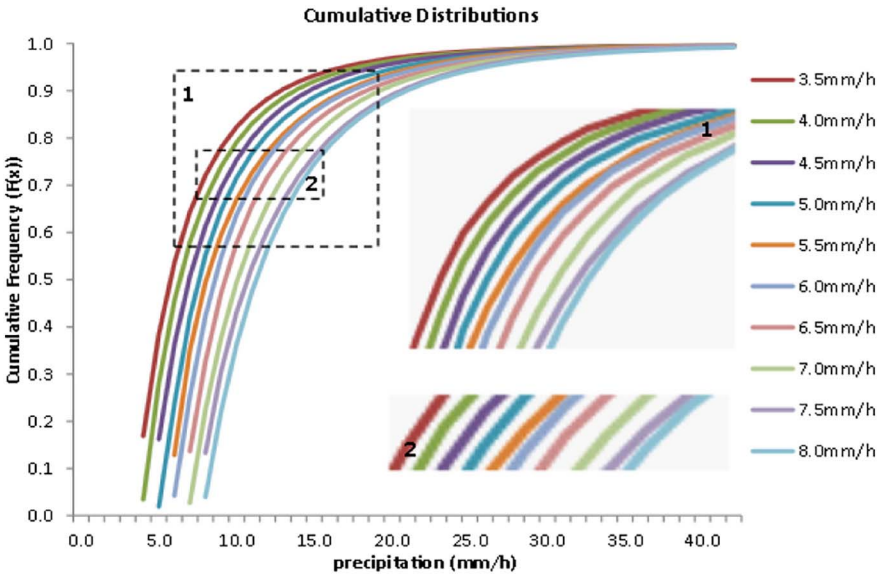

Fig. 2. Illustration of the cumulative distribution for each candidate hourly threshold. The x and y axis represent, the precipitation in mm/h and the cumulative frequency, respectively. The areas with the greatest concern and interest are enlarged in the frames 1 and 2.

absolute deviations between the coefficients of x (Δx), contribute decisively to the conduct of the results, comparing to differences of the ones of x^2 (Δx^2), which do not present a clear view, due to their small order of magnitude. In particular, the absolute deviation (0.010) observed between the coefficients of x of the 3rd order regression lines of the cumulative distributions of the 4.5 mm/h and the 5.0 mm/h data sets, is worth-noting. Interestingly, the difference between the coefficients of x of the 3rd order regression lines of the curves of the 7.5 mm/h and the 8.0 mm/h data sets, is 0.009. However, the maximum absolute deviation (0.013) occurs between the coefficients of x of the 3rd order trendlines of the cumulative distributions of the 6.5 mm/h and the 7.0 mm/h data sets. Moreover, the signal given by the absolute deviation between the coefficients of x^2 of the aforementioned candidate hourly thresholds appears to be similar, since it takes the greater of the two values shown in the specific column (Δx^2) of Table 3. Finally, concerning the coefficients of x^3, they are approximate 0 for each studied hourly threshold, as well as the absolute deviations derived from them (Δx^3). Therefore, ***the value of 6.5 mm/h is deterministically defined as the hourly threshold of extreme precipitation in Thessaloniki, during the period 1947–2003***.

Table 2
Calculated coefficients of determination (R^2) of the 2nd, 3rd and 4th polynomial trendlines of the cumulative distributions for each candidate hourly threshold.

Candidate thresholds	R^2		
	2nd order	**3rd order**	**4th order**
3.5 mm/h	0.730	0.916	0.916
4.0 mm/h	0.803	0.881	0.893
4.5 mm/h	0.824	0.902	0.916
5.0 mm/h	0.837	0.859	0.891
5.5 mm/h	0.867	0.887	0.916
6.0 mm/h	0.850	0.855	0.901
6.5 mm/h	0.871	0.874	0.920
7.0 mm/h	0.853	0.856	0.924
7.5 mm/h	0.886	0.890	0.948
8.0 mm/h	0.847	0.864	0.939

According to the Fig. 5, the absolute deviations between the coefficients of the 2nd, 3rd and 4th order polynomial regressions (Fig. 5a, b and c, respectively) converge qualitatively to the same result, while they diverge quantitatively due to the different number of independent

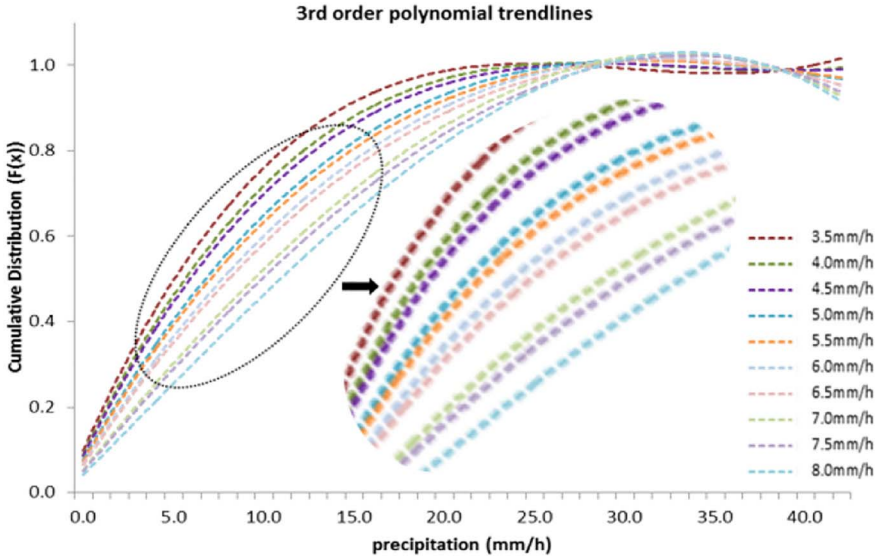

Fig. 3. Illustration of the 3rd order polynomial trendlines of the cumulative distributions for each candidate hourly threshold. The x and y axes represent, the precipitation in mm/h and the cumulative frequency, respectively. The region of the graph with the most pronounced differences between the curves is enlarged.

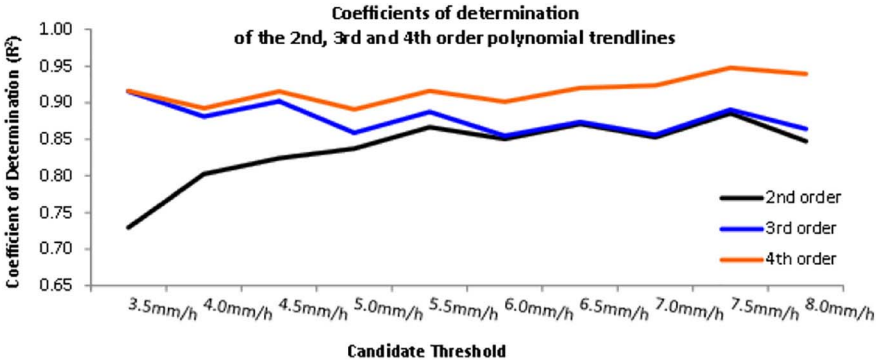

Fig. 4. Illustration of the coefficients of determination (R^2) of the 2nd, 3rd and 4th order polynomial trendlines of the cumulative distributions for each candidate hourly threshold. The x and y axis represent, the candidate threshold and the coefficient of determination, respectively.

Table 3
The coefficients of the independent variables of the 3rd order polynomial trendlines of the cumulative distributions (α_{ij}), as well as the calculated differences between the successive coefficients (Δ). The biggest difference is emphasized with bold.

Candidate threshold	α_{ij}			$\Delta = \lvert\alpha_{(i+1)j} - \alpha_{ij}\rvert$		
	x^3	x^2	x	Δx^3	Δx^2	Δx
3.5 mm/h	0.000	− 0.003	0.102	–	–	–
4.0 mm/h	0.000	− 0.003	0.093	0.000	0.001	0.009
4.5 mm/h	0.000	− 0.003	0.089	0.000	0.000	0.004
5.0 mm/h	0.000	− 0.002	0.079	0.000	0.001	0.010
5.5 mm/h	0.000	− 0.002	0.076	0.000	0.000	0.003
6.0 mm/h	0.000	− 0.001	0.069	0.000	0.000	0.007
6.5 mm/h	0.000	− 0.001	0.066	0.000	0.000	0.003
7.0 mm/h	0.000	− 0.001	0.054	0.000	**0.001**	**0.013**
7.5 mm/h	0.000	0.000	0.051	0.000	0.000	0.003
8.0 mm/h	0.000	0.000	0.042	0.000	0.001	0.009

variables participating in each figure. Nevertheless, owing to their very small order of magnitude, the absolute deviations (Δx^3 and Δx^4) of the coefficients of x^3 and x^4, appear to be completely absent from the graphical illustration (yellow and purple shading, correspondingly), indicating their negligible quantitative contribution to the result. This last notation validates the unnecessary use of the 4th order polynomial trendlines in the particular study.

To sum up, as shown in Fig. 6, the value of the threshold to be selected should not be very high, because the sample size decreases rapidly, resulting in invalid conclusions. On the other hand, the selection of a relatively small threshold can lead to a strong autocorrelation of the data, thus rejecting a possible theoretical model that could adequately describe the tails of the distribution (Wilks, 2006). The threshold of 6.5 mm/h, selected in this particular study, corresponds to 93% of the total rainfall data (daily precipitation ≥ 0.1 mm). This fact ensures the detection of the really intense rainfall (7% of the upper tail) of the period 1947–2003 and renders the threshold of 6.5 mm/h as the best solution for determining the extreme precipitation in Thessaloniki.

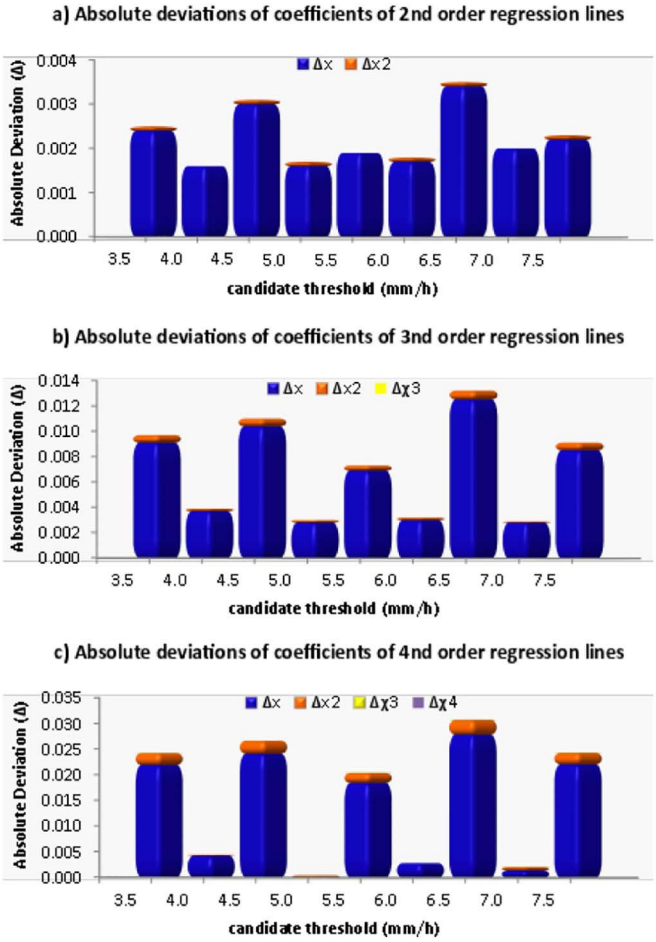

Fig. 5. Illustration of the absolute deviations of the coefficients of the a) 2nd, b) 3rd and c) 4th order polynomial trendlines of the cumulative distributions for each candidate hourly threshold. The x and y axis represent, the candidate threshold and the absolute deviation, respectively.

3.2. Identification of the best-fitted distribution of extreme precipitation in Thessaloniki

3.2.1. Annual best-fitted distribution

The data exceeding the hourly threshold of 6.5 mm/h were described by a set of 61 distributions exhibited in Appendix A, while the annual ranking of these theoretical distributions according to Kolmogorov-Smirnov, Anderson-Darling and Chi-Squared goodness-of-fit tests are presented in Appendix B, Table B.1.

The Johnson SB probability distribution, according to the Kolmogorov-Smirnov test and the Generalized Pareto, according to both Anderson-Darling and Chi-square tests, obtained the first rank for maximum hourly rainfall, annually. Interestingly, Generalized Pareto theoretical distribution appears to be in a very satisfactory rank of the 3rd position according to Kolmogorov-Smirnov test, whereas Johnson SB obtained the second and ninth rank by Anderson-Darling and Chi-Squared tests, respectively. Nevertheless, the interest lies in the selection of one from the two first rank models that predict to the most optimum extent the extreme hourly rainfall in Thessaloniki over the period 1947–2003.

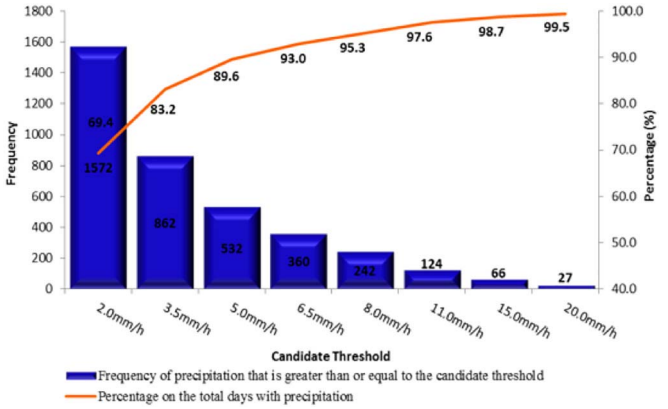

Fig. 6. Illustration of the frequency of precipitation that is greater than or equal to the candidate threshold (columns), as well as the percentage on the total days with precipitation (line). The x and y axis represent, the candidate threshold and the frequency, respectively.

A graphical comparison of the first rank models obtained by Kolmogorov-Smirnov test, and by both Anderson-Darling and Chi-Squared tests, is performed through the use of the probability function (a), the quantile plot (b) and the probability plot (c) (Fig. 7). Concerning the results from the quantile plot, the points of both models approximately lie on the line y = x, suggesting the very good fit of each model to the actual data. However, despite the weakness of the Generalized Pareto distribution to simulate the maximum hourly measurement (55,5 mm), the "orange" points are placed closer to the bisectrix of the first quadrant than the "blue" ones. This remark seems to be consistent with both Anderson-Darling and Chi-Squared analytical tests, since they converged on Generalized Pareto as the most descriptive distribution on annual basis.

On the other hand, being expressed on different scales, the information contained in both quantile and probability plots (Fig.7a and c), is identical. The above difference on the scale can significantly contribute to the outcome, as what appears to be as appropriate fit in one case may not be a particularly good fit in the other case. Characteristically, Fig. 7c presents perfect fit of both models to the empirical data. The diverging behavior of the most extreme rainfall values in the quantile plot does not totally coincide with this result, though. As far as the probability density functions of Johnson SB and Generalized Pareto distributions are concerned, both models show very good predictive abilities of the hourly extreme rainfall in Thessaloniki.

The selection of the best one from the two aforementioned models is based and fully done through their parameters presented in Table 4. Considering these values, in combination with the mathematical expressions of Johnson SB and Generalized Pareto distributions exhibited in Appendix A, the following types were produced for each model, respectively.

$$F(x) = \frac{1}{\sqrt{2\pi}} \int_0^{2.9242+0.87963\,ln\left(\frac{x-6.0626}{-x+97.5756}\right)} e^{-t^2/2} dt \quad (6)$$

$$F(x) = exp\left(-\left(1 + 0.19922\frac{x - 6.2947}{4.0384}\right)^{-1/0.19922}\right) \quad (7)$$

As it appears on the last column of Table 4, the absolute deviation, being calculated through the actual and estimated values according to Eq. (6), for the Johnson SB model is 40.9 units. On the other hand, the theoretical distribution indicated by Anderson-Darling and Chi-Squared goodness-of-fit tests presents, by far, the smallest absolute deviation (10.8). Therefore, the ***Generalized Pareto distribution is the most representative and descriptive model of the hourly extreme rainfall in Thessaloniki over the period 1947–2003, on annual basis.***

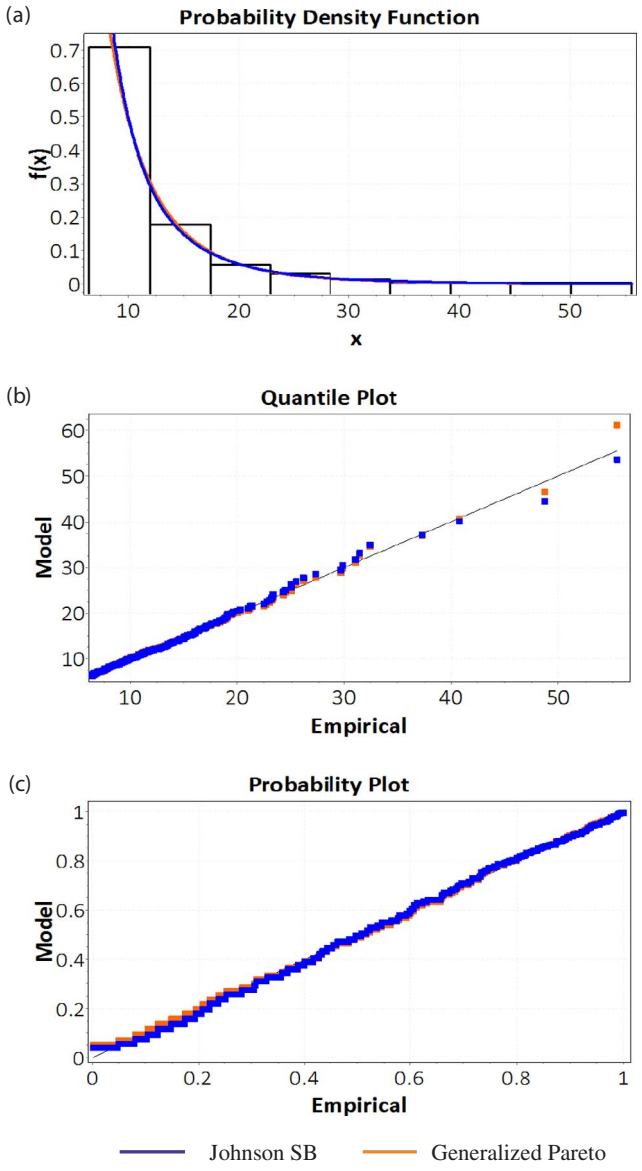

Fig. 7. Comparison of the first rank annual models obtained by Kolmogorov-Smirnov test (blue) and, Anderson-Darling and Chi-Squared tests (orange) by the use of the Probability Density Function (a), the Quantile Plot (b) and the Probability Plot (c). (For interpretation of the references to colour in this figure legend, the reader is referred to the web version of this article.)

Table 4
The parameters, as well as the absolute deviation between the actual and estimated values of extreme rainfall, of the first ranked probability distribution for each goodness-of-fit test, annually. The best fitted distribution along with its minimum absolute deviation, are emphasized with bold.

Goodness of fit test	Theor. distribution	Parameters				Absolute deviation
K-S	Johnson SB	γ	**δ**	**λ**	**ξ**	40.9
		2.9242	0.87963	91.513	6.0626	
A-D and X^2	**Gen. Pareto**	**k**	**σ**	**μ**		**10.8**
		0.19922	4.0384	6.2947		

3.2.2. Seasonal best-fitted distribution

Regarding the seasonal ranking of the sixty-one (61) theoretical distributions employed in the present study, they are presented in Appendix B: Table B.2, Table B.3, Table B.4 and Table B.5, for winter, spring, summer and autumn, respectively.

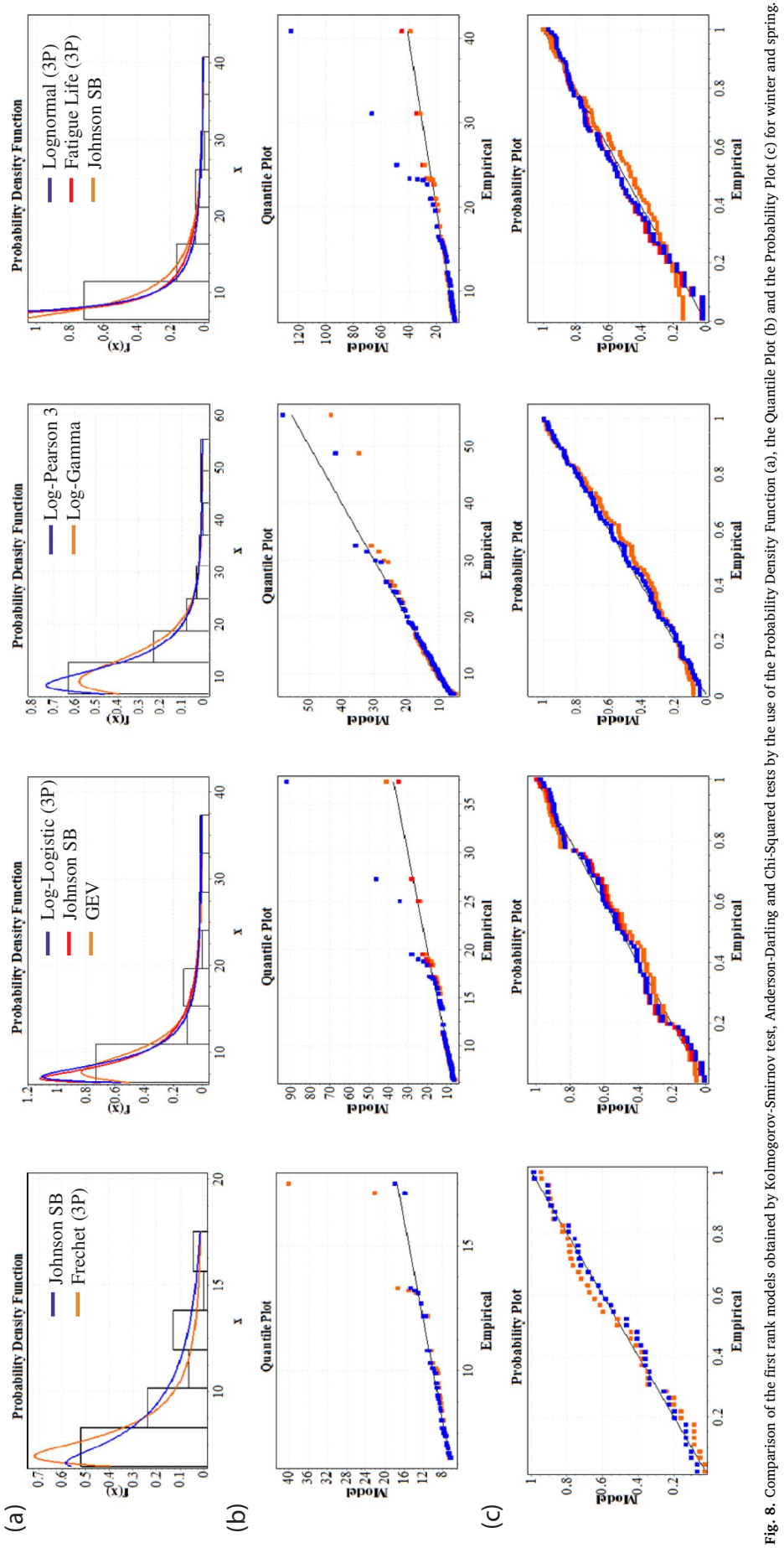

Fig. 8. Comparison of the first rank models obtained by Kolmogorov-Smirnov test, Anderson-Darling and Chi-Squared tests by the use of the Probability Density Function (a), the Quantile Plot (b) and the Probability Plot (c) for winter and spring.

Table 5
The parameters, as well as the absolute deviation between the actual and estimated values of extreme rainfall, of the first ranked probability distribution for each goodness-of-fit test, seasonally. The best fitted distribution along with its minimum absolute deviation, are emphasized with bold for each season.

Season	Goodness of fit test	Theor. distribution	Parameters				Absolute deviation
Winter	K-S and A-D	**Johnson SB**	γ	***δ***	**λ**	***ξ***	**12.1**
			1.5516	0.79413	16.408	6.1414	
	X^2	Frechet (3P)	***α***	***β***	γ		62.0
			1.5006	1.6926	5.7653		
	K-S	Log-Logistic (3P)	***α***	***β***	γ		81.5
Spring			1.4452	2.4442	6.4191		
	A-D	**Johnson SB**	γ	***δ***	**λ**	***ξ***	**29.1**
			2.4671	0.8264	54.933	6.2954	
	X^2	Gen. Extreme Value	***k***	***σ***	***μ***		35.3
			0.37791	2.0728	8.3101		
Summer	K-S and A-D	**Log-Pearson 3**	***α***	***β***	γ		**4.8**
			3.6988	0.2266	1.6106		
	X^2	Log-Gamma	***α***	***β***			156.7
			31.566	0.0776			
	K-S	Lognormal (3P)	***σ***	***μ***	γ		95.3
Autumn			1.675	0.47763	6.4564		
	A-D	**Fatigue Life (3P)**	***α***	***β***	γ		**26.1**
			1.7883	1.6621	6.3854		
	X^2	Johnson SB	γ	***δ***	**λ**	***ξ***	85.5
			2.2549	0.79684	54.919	5.6788	

In winter, Johnson SB distribution succeeded the first rank for the hourly extreme rainfall, according to both, Kolmogorov-Smirnov and Anderson-Darling analytical tests. On the other hand, the Chi-Squared goodness-of-fit test suggested the Frechet (3P) distribution as the most suitable model for the prediction of the maximum hourly rainfall in Thessaloniki. As it was previously used (Section 3.2.1), a graphical comparison of the first rank models obtained by both Kolmogorov-Smirnov test and Anderson-Darling tests, and Chi-Squared test, is demonstrated in the first column of Fig. 8. It is apparent from the graphs (a) and (b) that Johnson SB model can be easily characterized as the most representative distribution of the two. The weakness of Frechet (3P) to simulate the hourly extreme rainfall in winter is evident in both graphs. Characteristically, the most extreme hourly value of rainfall is overestimated above twice by the Frechet (3P) model (graph b). Concerning the probability plot (c), no clear difference between the two models was observed. In Table 5, the absolute deviation between the actual and estimated rainfall data of Johnson SB is approximately 12 units, while the absolute deviation between the actual and estimated extreme precipitation measurements of Frechet (3P) is almost 50 units higher, as it was expected. Consequently, ***for winter, the Johnson SB distribution is the most predictive model of the hourly extreme rainfall in Thessaloniki over the period 1947–2003.***

In spring, it has been observed that Log-Logistic (3P), Johnson SB and Generalized Extreme Value distributions obtained the first rank for maximum hourly rainfall by Kolmogorov-Smirnov, Anderson-Darling and Chi-Squared goodness-of-fit test, respectively. Surprisingly, none of the empirical tests of Fig. 7(a, b, c) seems to agree with each other. Specifically, the probability density functions of Log-Logistic (3P) and Johnson SB distributions behave in a similar way, contrasting to Generalized Extreme Value. On the other hand, in the quantile plot, Log-Logistic (3P) appears significantly diverging from the line y = x, whereas both Johnson SB and Generalized Extreme Value models tend to be placed on the diagonal. As far as the probability plot is concerned, no appreciable difference among the three distributions was found. In order to select the most representative model of the three, the calculated absolute deviations presented in Table 5, are of paramount importance in this particular case. The minimum absolute deviation is 29.1 units and corresponds to Johnson SB model that was proposed by Anderson-Darling goodness-of-fit test. Besides, one of the most attractive features of Anderson-Darling test is that more weight is given to the tails of the distribution. Concluding, ***in spring, the Johnson SB distribution is the most appropriate and representative model of the hourly extreme rainfall in Thessaloniki over the period 1947–2003.***

In summer, it has been observed that Log-Pearson 3 is the best-fitted model to extreme rainfall data according to both Kolmogorov-Smirnov and Anderson-Darling analytical tests. Furthermore, the Chi-Squared test indicated the two parameter theoretical distribution, Log-Gamma, as the most predictive model of maximum hourly rainfall in Thessaloniki over the studied period. As it can be seen from Fig. 8, a significant trend of underestimation of the highest hourly records by Log-Gamma model is detected in all graphs (a, b and c). This could be attributed to the fact that the satisfactory description of an extreme phenomenon, such as the extreme rainfall in an area, requires the use of the maximum possible information, which cannot be included in a two-parameter model. In addition, the Chi-Squared non-parametric test is often not the best goodness-of-test for continuous data, as it presupposes to group them, resulting in the loss of information. The above mentioned are supported through the absolute deviations calculated between the actual and estimated values of the extreme hourly rainfall (Table 5). In particular, it is noticed that the minimum absolute deviation (4.8 units) corresponds to Log-Pearson 3 model and is almost thirty-one (31) times smaller than the Log-Gamma's absolute deviation. Ending up, ***in summer, the Log-Pearson 3 distribution is the best-fitted model to the hourly extreme rainfall in Thessaloniki over the period 1947–2003.***

In autumn, the Lognormal (3P), Fatigue Life (3P) and Johnson SB models identified as the best fitted ones for Kolmogorov-Smirnov, Anderson-Darling and Chi-Squared non-parametric tests, respectively. The outcome taken from the quantile plot of the last column of the Fig. 8 seems to be different, though. The weakness of Lognormal (3P) to predict the over 23 mm/h values of extreme rainfall is evident. Interestingly, the absolute maximum measurement of precipitation recorded in Thessaloniki during 1967 is overestimated by almost eighty (80) units. On the contrary, it is observed that Fatigue Life (3P) and Johnson SB models simulate the empirical data satisfactorily. Regarding the probability density function (a) and the probability plot (c), no significant difference among the three models was found. Moreover, it is worth-noting that the probability density function contains less

Table 6
Estimated return levels (x_T) based upon fixed return periods on the left and estimated returns periods based upon the seven (7) most extreme precipitation events encountered for the period 1947–2003 on the right.

P (prob. of occurrence)	T (return period in years)	X_T (return level in mm/h)	P (prob. of occurrence)	T (return period in years)	Xm (return level in mm/h)
0.5	2	9.3	0.0014	720	55.5
0.2	5	14	0.0042	240	48.7
0.1	10	18.1	0.0069	144	40.8
0.05	20	22.8	0.0097	103	37.3
0.02	50	30.2	0.0125	80	32.5
0.01	100	36.8	0.0153	65	31.5
0.005	200	44.3	0.0181	55	31.1

information than the other two graphs, since the shape of histogram varies according to the number of classes, resulting in the assessment to be considered highly subjective. However, the selection of the best one of the models is accomplished through the calculated absolute deviations presented in Table 5. Specifically, it has been estimated that the absolute deviations between the actual and the calculated precipitation values are 95.3, 26.1 and 85.5 units for the Lognormal (3P), Fatigue Life (3P) and Johnson SB models, correspondingly. The minimum one is produced, for one more time, by the Anderson-Darling goodness-of-fit test. Therefore, ***in autumn, the Fatigue Life (3P) distribution is the most descriptive and predictive model of the hourly extreme rainfall in Thessaloniki over the period 1947–2003.***

3.3. Return levels and return periods

The derivation of the return levels of different precipitation extreme values is very important and of valuable interest. In the present study, the Generalized Pareto distribution was used (since it was proved, in Section 3.2.1, to be the best-fitted model for the annual data) to estimate the return levels (x_T) on annual basis for 2, 5, 10, 20, 50, 100 and 200 years (left side) and the return periods of the seven most extreme precipitation events (x_m) in Thessaloniki over the studied period (Table 6). In brief, it has been predicted that the rainfall of 9,3 mm/h or more, should occur at the studied location only once every two years, on the average. On the contrary, the return period of the most extreme precipitation event in Thessaloniki that occurred over the period 1947–2003 (that is 55,5 mm/h) is once every 720 years, approximately.

4. Conclusions

One of the main objectives of this study was to define and determine the most representative absolute hourly threshold of extreme precipitation events in Thessaloniki over the period 1947–2003. This was accomplished by obtaining the coefficients of the independent variables of the 3rd order polynomial trendlines of the cumulative distributions of ten (10) candidate datasets. The best fitted probability distribution of the rainfall data exceeding the selected hourly threshold were examined according to Kolmogorov-Smirnov, Anderson-Darling and Chi-Squared tests, on both annual and seasonal scale. Moreover, the annual return levels of some of the most extreme rainfall records are estimated and predicted.

- The value of 6.5 mm/h is, both visually and deterministically, defined as the hourly threshold of extreme precipitation in Thessaloniki, during the period 1947–2003 and it corresponds to 93% of the total rainfall data (daily precipitation ≥ 0.1 mm).
- The use of the 3rd order regression lines is deemed to be the most prudent option, as the coefficients of R^2 of the 2nd order polynomial trendlines present a weaker fit to the data of 50% of the candidate hourly thresholds. Conversely, despite the almost perfect fit to the data presented by the coefficients of R^2 of the 4th order regression lines, adding one more parameter is considered to be needless, since its contribution to the result is not observable.
- The determination of the hourly threshold of extreme precipitation is essentially based upon the differences between the coefficients of x of the 3rd order polynomial trendlines of the successive cumulative distributions of the ten data sets, as the absolute deviations between the corresponding coefficients of x^2 and x^3 are of very small order of magnitude.
- As far as the best-fitted models of the maximum hourly precipitation are concerned, the Generalized Pareto Distribution identified as the most representative one for the description of the annual extreme rainfall, while the Johnson SB, log-Pearson and Fatigue Life (3P) distributions satisfactorily predict the hourly data for winter and spring, summer, and autumn, respectively.
- Interestingly, the minimum absolute deviations between the actual and estimated values, being produced by generating random numbers from the parameters of the selected probability distributions, were mainly indicated by Anderson-Darling goodness-of-fit test, on both annual and seasonal scale. This could be attributed to the fact that this test gives more weight to the tails of the distribution comparing to the Kolmogorov-Smirnov and Chi-Squared tests. Therefore, the Anderson-Darling non-parametric test could be characterized as the most suitable goodness-of-fit test of the extreme precipitation data among the three. These are in accordance to Ahmad et al. (1988), who suggest that the Anderson-Darling test is an attractive and powerful mean of assessing goodness of fit on frequency models.
- In summer, an underestimation of the most extreme rainfall data has been observed by the best-fitted models, whereas in the rest of the seasons an overestimation of the maximum hourly measurements is noted by some of the first ranked models. This can be attributed to the fact that models often tend to underestimate heavy rainfalls, very cold or very hot temperatures, since their resolution and the numerical diffusion, which ensure their stability in long runs, limit the range of variations of their prognostic variables. This was also found and stated by Déqué (2007).
- Finally, despite the fact that the calculation of return levels and return periods involves uncertainties regarding the probabilistic outcomes, it has been shown that the knowledge of them, in local scale, could act as a useful tool for designing the appropriate infrastructures for prevention of damages.

Appendix A. Appendix A

No	Distribution	Probability Density Function	Range	Parameters
1	Fatigue Life (3P)	$f(x) = \frac{\sqrt{(x-\gamma)/\beta} + \sqrt{\beta/(x-\gamma)}}{2\alpha(x-\gamma)} \bullet \varphi\left(\frac{1}{\alpha}\left(\sqrt{\frac{(x-\gamma)}{\beta}} - \sqrt{\frac{\beta}{(x-\gamma)}}\right)\right)$, where $\varphi(x) = \frac{e^{-x^2/2}}{\sqrt{2\pi}}$	$\gamma < x < +\infty$	β: continuous scale parameter ($\beta > 0$) γ: continuous location parameter ($\gamma \equiv 0$ yields the 2P Fatigue Life distribution)
2	Frechet (3P)	$f(x) = \frac{\alpha}{\beta}\left(\frac{\beta}{x-\gamma}\right)^{\alpha+1} \exp\left(-\left(\frac{\beta}{x-\gamma}\right)^{a}\right)$	$\gamma < x < +\infty$	α: continuous shape parameter ($\alpha > 0$) β: continuous scale parameter ($\beta > 0$) γ: continuous location parameter ($\gamma \equiv 0$ yields the 2P Frechet distribution)
3	Generalized Extreme Value	$f(x) = \begin{cases} \frac{1}{\sigma}\exp(-(1+kz)^{-\frac{1}{k}})(1+kz)^{-1-\frac{1}{k}}, & k \neq 0 \\ \frac{1}{\sigma}\exp(-z-\exp(-z)), & k = 0 \end{cases}$, where $z \equiv \frac{x-\mu}{\sigma}$	$1 + k\frac{(x-\mu)}{\sigma} > 0, k \neq 0$ $-\infty < x < +\infty, \kappa = 0$	k: continuous shape parameter σ: continuous scale parameter ($\sigma > 0$) μ: continuous location parameter
4	Generalized Pareto	$f(x) = \begin{cases} \frac{1}{\sigma}(1 + k\frac{(x-\mu)}{\sigma})^{-1-1/\kappa}, & k \neq 0 \\ \frac{1}{\sigma}\exp(-\frac{(x-\mu)}{\sigma}), & k = 0 \end{cases}$, where $z \equiv \frac{x-\mu}{\sigma}$	$\mu \leq x < +\infty, k \geq 0$ $\mu \leq x \leq \mu - \sigma/k, \kappa < 0$	k: continuous shape parameter σ: continuous scale parameter ($\sigma > 0$) μ: continuous location parameter
5	Johnson SB	$f(x) = \frac{\delta}{\lambda\sqrt{2\pi}\, z\,(1-z)} \exp\left(-\frac{1}{2}\left(\gamma + \delta \ln\left(\frac{z}{1-z}\right)\right)^2\right)$, where $z \equiv \frac{x-\mu}{\sigma}$	$\xi \leq x \leq \xi + \lambda$	γ: continuous shape parameter δ: continuous shape parameter ($\delta > 0$) λ: continuous scale parameter ($\lambda > 0$) ξ: continuous location parameter
6	Log-Gamma	$f(x) = \frac{(\ln(x))^{\alpha-1}}{x\beta^{\alpha}\Gamma(\alpha)} \exp(-\ln(x)/\beta)$	$0 < x < +\infty$	α: continuous parameter ($\alpha > 0$) β: continuous parameter ($\beta > 0$)
7	Log-Logistic (3P)	$f(x) = \frac{\alpha}{\beta}\left(\frac{x-\gamma}{\beta}\right)^{\alpha-1}\left(1 + \left(\frac{x-\gamma}{\beta}\right)^{\alpha}\right)^{-2}$	$\gamma \leq x < +\infty$	α: continuous shape parameter ($\alpha > 0$) β: continuous scale parameter ($\beta > 0$) γ: continuous location parameter ($\gamma \equiv 0$ yields the 2P Log-Logistic distribution)
8	Log-Pearson 3	$f(x) = \frac{1}{x\,\lvert\beta\rvert\,\Gamma(\alpha)}\left(\frac{\ln(x)-\gamma}{\beta}\right)^{\alpha-1}\exp\left(-\frac{\ln(x)-\gamma}{\beta}\right)$	$0 < x \leq e^{\gamma}, \beta < 0$ $e^{\gamma} \leq x < +\infty, \beta > 0$	α: continuous parameter ($\alpha > 0$) β: continuous parameter ($\beta \neq 0$) γ: continuous parameter
9	Lognormal (3P)	$f(x) = \frac{\exp\left(-\frac{1}{2}\left(\frac{\ln(x-\gamma)-\mu}{\sigma}\right)^2\right)}{(x-\gamma)\,\sigma\,\sqrt{2\pi}}$	$\gamma < x < +\infty$	σ: continuous parameter ($\sigma > 0$) μ: continuous parameter γ: continuous location parameter ($\gamma \equiv 0$ yields the 2P Lognormal distribution)

Appendix B. Appendix B

Table B.1
Annual rank of the theoretical distributions used in the particular study, as well as their test statistics, according to Kolmogorov-Smirnov, Anderson-Darling and Chi-Squared tests. The probability distributions in which the goodness of fit test is not applicable appear as N/A, while “No fit” is interpreted as the unfitness of the distribution to describe the data. The best fitted probability distribution for each goodness-of-fit test is emphasized with different colour.

Distribution		Kolmogorov-Smirnov		Anderson-Darling		Chi-Squared	
		Statistic	Rank	Statistic	Rank	Statistic	Rank
1	Beta	0,10102	18	15,564	23	47,655	27
2	Burr	N/A		N/A		N/A	
3	Burr (4P)	0,09275	16	69,243	47	N/A	
4	Cauchy	0,22762	43	26,911	33	72,987	37
5	Chi-Squared	0,16199	28	12,877	19	31,235	22
6	Chi-Squared (2P)	0,10533	20	14,731	21	54,404	28
7	Dagum	0,95476	56	1123,700	56	12161,000	50
8	Dagum (4P)	0,10268	19	16,484	26	20,868	15
9	Erlang	0,30380	48	27,397	37	79,075	38
10	Erlang (3P)	No fit					
11	Error	0,22347	39	27,193	35	83,554	39
12	Error Function	0,85344	55	581,780	55	2170,600	49
13	Exponential	0,43634	50	63,650	43	223,620	44
14	Exponential (2P)	0,08981	15	29,953	41	21,199	16
15	Fatigue Life	0,13462	27	11,697	17	29,145	21
16	Fatigue Life (3P)	0,05503	8	1272	3	6174	3
17	Frechet	0,09591	17	3356	11	13,049	10
18	Frechet (3P)	0,05583	10	2142	7	17,661	13
19	Gamma	0,22854	44	18,265	28	54,784	29
20	Gamma (3P)	0,05151	7	11,771	18	5583	2
21	Generalized Extreme Value	0,07777	13	2654	9	9549	8
22	Generalized Gamma	0,16395	29	16,105	24	41,952	25
23	Generalized Gamma (4P)	0,06935	12	16,242	25	6681	5
24	**Generalized pareto**	0,04932	3	**0648**	**1**	**5358**	**1**
25	Gumbel max	0,21619	36	16,952	27	38,280	24
26	Gumbel min	0,26076	45	60,946	42	N/A	
27	Hypersecant	0,19891	33	24,859	31	58,579	30
28	Inversion Gaussian	0,20853	34	13,781	20	47,578	26
29	Inversion Gaussian (3P)	0,05048	6	1527	4	8235	6
30	**Johnson SB**	**0,03822**	**1**	0659	2	9765	9
31	Johnson SU	No fit					
32	Kumaraswamy	0,22052	38	92,640	49	N/A	
33	Laplace	0,22347	40	27,193	36	83,554	40
34	Levy	0,44082	53	116,020	52	458,180	47
35	Levy (2P)	0,17187	30	14,832	22	98,514	41
36	Log-Gamma	0,12415	24	7466	12	26,461	17
37	Log-Logistic	0,12854	25	9921	15	28,375	18
38	Log-Logistic (3P)	0,04989	5	2871	10	19,643	14
39	Log-Pearson 3	0,08495	14	2373	8	6419	4
40	Logistic	0,19491	32	25,062	32	65,793	33
41	Lognormal	0,12899	26	10,394	16	37,645	23
42	Lognormal (3P)	0,04946	4	1652	5	13,731	11
43	Nakagami	No fit					
44	Normal	0,21697	37	29,164	39	66,519	35
45	Pareto	0,04722	2	29,856	40	8759	7
46	Pareto 2	0,43914	51	64,464	45	216,480	43
47	Pearson 5	0,10767	21	7550	13	28,854	20
48	Pearson 5 (3P)	0,05522	9	2058	6	15,581	12
49	Pearson 6	0,10791	22	7632	14	28,834	19
50	Pearson 6 (4P)	0,11094	23	72,661	48	N/A	
51	Pert	0,29472	47	93,587	50	164,250	42
52	Power Function	0,36013	49	65,151	46	374,160	45
53	Rayleigh	0,22752	42	21,313	29	60,993	32
54	Rayleigh (2P)	0,21424	35	28,234	38	71,444	36
55	Reciprocal	0,43946	52	199,130	53	414,330	46
56	Rice	0,22392	41	21,804	30	65,863	34
57	Student's t	0,98857	57	1420,700	57	26127,00	51
58	Triangular	0,51531	54	287,190	54	714,850	48
59	Uniform	0,27412	46	109,140	51	N/A	
60	Weibull	0,18035	31	27,131	34	59,648	31
61	Weibull (3P)	0,05598	11	64,335	44	N/A	

Table B.2
As in Table B.1, but for winter.

Distribution		Kolmogorov-Smirnov		Anderson-Darling		Chi-Squared	
		Statistic	Rank	Statistic	Rank	Statistic	Rank
1	Beta	0,14315	21	8878	47	N/A	
2	Burr	0,10377	12	33,335	57	N/A	
3	Burr (4P)	0,13550	19	8288	45	N/A	
4	Cauchy	0,23465	46	3810	41	11,783	42
5	Chi-Squared	0,31098	51	3969	42	2,9157	22
6	Chi-Squared (2P)	0,37461	54	16,345	54	30,890	50
7	Dagum	0,29291	50	8735	46	20,004	45
8	Dagum (4P)	0,15818	25	2467	32	2369	14
9	Erlang	0,19909	37	1650	22	0980	2
10	Erlang (3P)	0,10514	14	2025	26	3074	24
11	Error	0,22310	43	2737	35	9250	40
12	Error Function	0,99217	59	243,440	59	9445,100	53
13	Exponential	0,51163	55	11,963	52	24,803	48
14	Exponential (2P)	0,10514	13	3096	38	3074	23
15	Fatigue Life	0,16868	31	1544	21	2233	12
16	Fatigue Life (3P)	0,10293	11	0438	3	2440	17
17	Frechet	0,11275	17	0692	10	3355	27
18	**Frechet (3P)**	0,09577	8	0586	7	**0921**	**1**
19	Gamma	0,16788	30	1667	23	2709	21
20	Gamma (3P)	0,14099	20	9099	49	N/A	
21	Generalized Extreme Value	0,11130	16	0654	9	3655	28
22	Generalized Gamma	0,16964	32	1766	24	3844	29
23	Generalized Gamma (4P)	0,11007	15	2020	25	2406	16
24	Generalized Pareto	0,07581	2	0358	2	1459	7
25	Gumbel max	0,14783	22	1215	12	2620	20
26	Gumbel min	0,23554	47	6130	44	11,990	43
27	Hypersecant	0,20937	39	2532	33	9035	39
28	Inversion Gaussian	0,15982	27	1390	17	1449	5
29	Inversion Gaussian (3P)	0,09638	9	0517	5	2115	11
30	**Johnson SB**	**0,07254**	**1**	**0319**	**1**	1449	6
31	Johnson SU			No fit			
32	Kumaraswamy	0,08191	3	1453	18	2519	19
33	Laplace	0,23680	48	3002	37	11,991	44
34	Levy	0,53189	56	17,748	56	58,865	51
35	Levy (2P)	0,21184	40	2122	27	10,119	41
36	Log-Gamma	0,15348	24	1234	13	3237	25
37	Log-Logistic	0,15025	23	1291	15	3989	31
38	Log-Logistic (3P)	0,08586	5	0587	8	1207	3
39	Log-Pearson 3	0,12102	18	0707	11	2501	18
40	Logistic	0,19462	36	2380	30	7828	38
41	Lognormal	0,16635	29	1507	19	3277	26
42	Lognormal (3P)	0,08697	6	0482	4	2297	13
43	Nakagami	0,22433	45	2187	29	1315	4
44	Normal	0,17629	34	2390	31	6306	35
45	Pareto	0,08383	4	3747	40	2402	15
46	Pareto2	0,59552	57	16,885	55	24,115	47
47	Pearson 5	0,16148	28	1307	16	4007	32
48	Pearson 5 (3P)	0,09819	10	0582	6	1812	9
49	Pearson 6	0,15832	26	1280	14	3883	30
50	Pearson 6 (4P)	0,18658	35	9157	50	N/A	
51	Pert			No fit			
52	Powerfunction	0,21935	42	3215	39	7488	36
53	Rayleigh	0,33196	53	4952	43	5480	34
54	Rayleigh (2P)	0,21381	41	2561	34	7580	37
55	Reciprocal	0,31780	52	13,301	53	27,478	49
56	Rice	0,20656	38	2143	28	1665	8
57	Student's t	0,98857	58	173,810	58	2984,100	52
58	Triangular	0,28099	49	9040	48	21,422	46
59	Uniform	0,22423	44	9695	51	N/A	
60	Weibull	0,17606	33	2803	36	4008	33
61	Weibull (3P)	0,08843	7	1534	20	1821	10

Table B.3
As in Table B.1, but for spring.

Distribution		Kolmogorov-Smirnov		Anderson-Darling		Chi-Squared	
		Statistic	Rank	Statistic	Rank	Statistic	Rank
1	Beta	0,14,419	19	3468	17	21,364	26
2	Burr	0,14,793	23	9481	44	N/A	
3	Burr (4P)	0,15,897	24	9698	45	N/A	
4	Cauchy	0,19,559	30	6362	27	14,305	15
5	Chi-Squared	0,22,835	38	4723	24	31,720	38
6	Chi-Squared (2P)	0,17,998	27	7012	35	14,268	14
7	Dagum	0,57,277	57	81,735	57	211,660	48
8	Dagum (4P)	0,12,507	17	8802	43	N/A	
9	Erlang	0,27,999	48	6506	29	38,582	41
10	Erlang (3P)	No fit					
11	Error	0,26,556	46	7854	38	30,316	35
12	Error Function	0,89,844	58	183,910	58	799,550	49
13	Exponential	0,45,445	53	17,451	51	73,768	43
14	Exponential (2P)	0,11,131	14	2518	12	9059	12
15	Fatigue Life	0,17,784	26	3748	19	22,936	28
16	Fatigue Life (3P)	0,08523	10	0508	6	10,225	13
17	Frechet	0,09241	11	1241	10	8580	10
18	Frechet (3P)	0,07870	5	0488	5	6013	5
19	Gamma	0,21,015	35	4880	25	33,258	39
20	Gamma (3P)	0,20,048	33	7814	37	20,423	23
21	**Generalized extreme value**	0,08509	9	0741	8	**2121**	**1**
22	Generalized Gamma	0,19,724	31	4690	23	24,204	30
23	Generalized Gamma (4P)	0,11,452	16	1599	11	7012	8
24	Gen. Pareto	0,07605	2	8210	40	N/A	
25	Gumbel Max	0,19,732	32	4413	21	25,509	31
26	Gumbel Min	0,30,080	50	14,361	49	28,848	33
27	Hypersecant	0,24,498	41	6857	32	20,699	24
28	Inversion Gaussian	0,19,374	29	3,931	20	29,652	34
29	Inversion Gaussian (3P)	0,07916	6	0469	2	6861	7
30	**Johnson SB**	0,07842	3	**0445**	**1**	4803	3
31	Johnson SU	No fit					
32	Kumaraswamy	0,18,196	28	13,714	48	N/A	
33	Laplace	0,26,556	47	7854	39	30,316	36
34	Levy	0,47,700	56	29,590	54	122,780	47
35	Levy (2P)	0,21,191	36	4950	26	31,384	37
36	Log-Gamma	0,14,514	21	2676	13	18,566	19
37	Log-Logistic	0,14,789	22	3076	16	16,240	16
38	**Log-Logistic (3P)**	**0,07067**	**1**	0547	7	8135	9
39	Log-Pearson 3	0,08149	8	0877	9	5836	4
40	Logistic	0,23,859	40	6700	31	19,461	20
41	Lognormal	0,16,633	25	3481	18	19,773	21
42	Lognormal (3P)	0,07861	4	0482	3	3762	2
43	Nakagami	0,37,635	51	11,265	46	52,819	42
44	Normal	0,23,100	39	6960	34	21,815	27
45	Pareto	0,11,336	15	4425	22	8779	11
46	Pareto 2	0,45,760	54	17,674	52	74,456	44
47	Pearson 5	0,14,350	18	2709	14	16,411	17
48	Pearson 5 (3P)	0,07955	7	0487	4	6014	6
49	Pearson 6	0,14,504	20	2783	15	16,418	18
50	Pearson 6 (4P)	0,10,982	13	8786	42	N/A	
51	Pert	0,29,339	49	12,744	47	26,679	32
52	Power Function	0,20,806	34	15,837	50	N/A	
53	Rayleigh	0,25,053	42	6526	30	20,107	22
54	Rayleigh (2P)	0,25,753	43	7419	36	24,031	29
55	Reciprocal	0,44,195	52	37,065	55	91,510	45
56	Rice	0,25,917	44	6425	28	33,952	40
57	Student's t	0,98,857	59	337,580	59	7360,800	50
58	Triangular	0,47,621	55	44,507	56	111,290	46
59	Uniform	0,26,109	45	18,663	53	N/A	
60	Weibull	0,21,549	37	6865	33	21,206	25
61	Weibull (3P)	0,10,917	12	8606	41	N/A	

Table B.4
As in Table B.1, but for summer.

Distribution		Kolmogorov-Smirnov		Anderson-Darling		Chi-Squared	
		Statistic	Rank	Statistic	Rank	Statistic	Rank
1	Beta	0,12,025	25	22,847	45	N/A	
2	Burr	0,08518	18	1002	10	9147	18
3	Burr (4P)	0,09277	19	20,006	42	N/A	
4	Cauchy	0,19,547	40	6750	28	13,497	25
5	Chi-Squared	0,11,119	23	3112	17	10,677	22
6	Chi-Squared (2P)	0,08486	17	3291	18	10,348	21
7	Dagum	0,32,426	49	34,692	49	66,801	40
8	Dagum (4P)	0,17,752	33	11,706	39	18,529	30
9	Erlang	0,44,439	54	37,592	52	80,441	42
10	Erlang (3P)	No fit					
11	Error	0,21,079	42	8308	33	23,383	34
12	Error Function	0,80,804	56	187,390	56	598,190	47
13	Exponential	0,39,540	51	20,682	43	77,110	41
14	Exponential (2P)	0,05325	10	6061	24	2811	7
15	Fatigue Life	0,11,304	24	2611	16	7658	17
16	Fatigue Life (3P)	0,05748	11	0,300	3	1803	3
17	Frechet	0,04989	6	0,349	5	4200	10
18	Frechet (3P)	0,04808	4	0,409	8	5188	13
19	Gamma	0,19,390	38	5449	23	15,535	29
20	Gamma (3P)	0,05748	12	19,463	41	N/A	
21	Generalized Extreme Value	0,05012	7	0,363	6	5109	12
22	Generalized Gamma	0,13,688	27	4408	20	12,386	23
23	Generalized Gamma (4P)	0,15,643	30	7069	29	13,918	26
24	Generalized Pareto	0,05213	9	19,404	40	N/A	
25	Gumbel Max	0,18,433	36	5096	22	14,187	28
26	Gumbel Min	0,24,535	46	21,197	44	N/A	
27	Hypersecant	0,18,956	37	7800	30	24,181	36
28	Inversion Gaussian	0,16,174	31	3600	19	12,677	24
29	Inversion Gaussian (3P)	0,05046	8	0,286	2	2599	5
30	Johnson SB	0,09628	21	32,547	48	N/A	
31	Johnson SU	No fit					
32	Kumaraswamy	0,21,530	45	29,057	47	N/A	
33	Laplace	0,21,079	43	8308	34	23,383	35
34	Levy	0,43,042	53	39,575	53	179,080	46
35	Levy (2P)	0,21,293	44	8403	35	53,758	39
36	**Log-Gamma**	0,08310	16	1289	13	**1445**	**1**
37	Log-Logistic	0,09581	20	1856	14	6743	16
38	Log-Logistic (3P)	0,04615	2	0507	9	3899	9
39	**Log-Pearson 3**	**0,04522**	**1**	**0264**	**1**	3009	8
40	Logistic	0,18,286	35	8004	31	29,276	37
41	Lognormal	0,10,192	22	2174	15	5217	14
42	Lognormal (3P)	0,04817	5	0,310	4	2664	6
43	Nakagami	No fit					
44	Normal	0,19,499	39	8953	37	30,084	38
45	Pareto	0,13,149	26	11,345	38	9554	19
46	Pareto 2	0,42,291	52	23,675	46	83,047	43
47	Pearson 5	0,07936	14	1211	11	1959	4
48	Pearson 5 (3P)	0,04665	3	0,371	7	5326	15
49	Pearson 6	0,08018	15	1231	12	1511	2
50	Pearson 6 (4P)	0,15,514	29	8161	32	9747	20
51	Pert	No fit					
52	Power Function	0,28,532	48	35,339	50	N/A	
53	Rayleigh	0,18,034	34	6075	25	19,767	31
54	Rayleigh (2P)	0,20,205	41	8579	36	20,413	32
55	Reciprocal	0,38,870	50	44,526	54	88,790	44
56	Rice	0,17,318	32	6617	26	21,300	33
57	Student's t	0,98,857	57	538,210	57	11,831,000	48
58	Triangular	0,46,050	55	69,834	55	148,630	45
59	Uniform	0,25,184	47	36,052	51	N/A	
60	Weibull	0,15,405	28	6728	27	14,115	27
61	Weibull (3P)	0,06490	13	4773	21	4262	11

Table B.5
As in Table B.1, but for autumn.

Distribution		Kolmogorov-Smirnov		Anderson-Darling		Chi-Squared	
		Statistic	Rank	Statistic	Rank	Statistic	Rank
1	Beta	0,12,092	12	30,468	46	N/A	
2	Burr	0,12,378	13	38,090	53	N/A	
3	Burr (4P)	0,11,803	11	11,644	39	6635	15
4	Cauchy	0,26,950	45	11,660	40	28,142	41
5	Chi-Squared	0,22,835	34	5084	19	8839	18
6	Chi-Squared (2P)	0,17,892	30	10,383	37	22,848	37
7	Dagum	0,85,858	56	162,800	57	635,240	51
8	Dagum (4P)	0,16,556	24	34,650	52	N/A	
9	Erlang	0,33,036	50	8162	29	5945	11
10	Erlang (3P)	No fit					
11	Error	0,26,022	43	9199	32	31,106	42
12	Error Function	0,86,478	57	156,270	56	485,530	50
13	Exponential	0,45,090	54	17,201	43	25,575	40
14	Exponential (2P)	0,17,420	28	25,911	45	18,698	34
15	Fatigue Life	0,17,437	29	4922	18	12,415	25
16	**FatigueLife(3P)**	0,07660	2	**0813**	**1**	2813	3
17	Frechet	0,15,205	17	2276	10	5543	10
18	Frechet (3P)	0,08462	5	1099	4	4343	6
19	Gamma	0,24,895	41	5816	21	8073	16
20	Gamma (3P)	0,16,988	26	10,273	35	13,342	29
21	Generalized Extreme Value	0,11,471	9	1854	8	6360	14
22	Generalized Gamma	0,18,969	31	5857	22	12,762	26
23	Generalized Gamma (4P)	0,08163	3	7850	27	4345	7
24	Generalized Pareto	0,11,505	10	1153	6	2951	4
25	Gumbel Max	0,23,607	38	5576	20	8755	17
26	Gumbel Min	0,28,206	47	18,252	44	34,352	44
27	Hypersecant	0,23,194	36	8289	30	23,154	38
28	Inversion Gaussian	0,23,373	37	4669	17	5314	9
29	Inversion Gaussian (3P)	0,09507	8	1061	3	4595	8
30	**JohnsonSB**	0,13960	14	1432	7	**2328**	**1**
31	Johnson SU	No fit					
32	Kumaraswamy	0,17,330	27	33,185	49	N/A	
33	Laplace	0,26,022	44	9,199	33	31,106	43
34	Levy	0,43,669	52	31,613	47	75,957	47
35	Levy (2P)	0,14,300	16	2,405	11	10,142	19
36	Log-Gamma	0,16,177	22	3,593	12	10,280	21
37	Log-Logistic	0,16,869	25	4,112	15	11,757	24
38	Log-Logistic (3P)	0,15,386	20	10,676	38	16,985	33
39	Log-Pearson 3	0,13,965	15	1,984	9	6,023	12
40	Logistic	0,22,235	33	8,141	28	21,393	35
41	Lognormal	0,16,468	23	4,557	16	13,523	30
42	**Lognormal (3P)**	**0,07289**	**1**	1047	2	2811	2
43	Nakagami	No fit					
44	Normal	0,23,077	35	8439	31	16,814	32
45	Pareto	0,09212	6	13,485	41	11,254	23
46	Pareto 2	0,43,991	53	16,564	42	22,410	36
47	Pearson 5	0,15,255	18	3790	13	12,949	28
48	Pearson 5 (3P)	0,09384	7	1137	5	4171	5
49	Pearson 6	0,15,437	21	3856	14	12,940	27
50	Pearson 6 (4P)	0,15,256	19	34,350	51	N/A	
51	Pert	0,31,992	49	32,793	48	62,031	46
52	Power Function	0,28,016	46	10,288	36	41,407	45
53	Rayleigh	0,24,591	40	6728	23	10,338	22
54	Rayleigh (2P)	0,24,912	42	9553	34	24,811	39
55	Reciprocal	0,42,253	51	60,118	54	118,240	48
56	Rice	0,24,267	39	6836	24	10,220	20
57	Student's t	0,98,857	58	377,010	58	5582,500	52
58	Triangular	0,46,397	55	76,664	55	161,710	49
59	Uniform	0,28,744	48	33,682	50	N/A	
60	Weibull	0,20,279	32	7761	26	15,627	31
61	Weibull (3P)	0,08433	4	7086	25	6321	13

References

Ahmad, M.I., Sinclair, C.D., Spurr, B.D., 1988. Assessment of flood frequency models using empirical distribution function statistics. Water Resour. Res. 24 (8), 1323–1328.

Anagnostopoulou, C., Tolika, K., 2010. Definition of extreme precipitation thresholds in Europe using parametric statistical methods. In: 10th COMECAP Conf. Proc, pp. 649–656.

Anagnostopoulou, C., Tolika, K., 2012. Extreme precipitation in Europe: statistical threshold selection based on climatological criteria. Theor. Appl. Climatol. 107, 479–489.

Bocheva, L., Marinova, T., Simeonov, P., Gospodinov, I., 2009. Variability and trends of extreme precipitation events over Bulgaria (1961–2005). Atmos. Res. 93, 490–497.

Bocheva, L., Gospodinov, I., Simeonov, P., Marinova, T., 2010. Climatological analysis of the synoptic situations causing torrential precipitation events in Bulgaria during the period 1961–2007. In: Alexandrov, V., Knight, C.G., Gajdusek, M.F., Yotova, A. (Eds.), Global Environmental Change: Challenges to Science and Society in Southeastern Europe. Springer, pp. 97–108 (ch. 9).

Chakravarti, I.M., Laha, R.G., Roy, J., 1967. Handbook of Methods of Applied Statistics. vol. I. John Wiley and Sons, pp. 392–394.

Chu, P.S., Zhao, X., Ruan, Y., Grubbs, M., 2009. Extreme rainfall events in the Hawaiian islands. J. Appl. Meteorol. Climatol. Am. Meteor. Soc. 48, 502–516.

Déqué, M., 2007. Frequency of precipitation and temperature extremes over France in an anthropogenic scenario: model results and statistical correction according to observed values. Glob. Planet. Chang. 57, 16–26.

Feng, S., Nadarajah, S., Hu, 2007. Modeling extreme precipitation in China using the generalized extreme value distribution. J. Meteorol. Soc. Jpn. 85, 599–613.

Fernández-Montes, S., Seubert, S., Rodrigo, F.S., Rasilla Álvarez, D.F., Hertig, E., Esteban, P., Philipp, A., 2014. Circulation types and extreme precipitation days in the Iberian peninsula in the transition seasons: spatial links and temporal changes. Atmos. Res. 138, 41–58.

Fujibe, F., Yamazaki, N., Katsurayama, M., Kobayashi, K., 2005. The increasing trend of intense precipitation in Japan based on four-hourly data for a hundred years. SOLA 1, 41–44. http://dx.doi.org/10.2151/sola. (2005–012).

Gao, M., Mo, D., Wu, X., 2016. Nonstationary modeling of extreme precipitation in China. Atmos. Res. 182, 1–9. http://dx.doi.org/10.1016/j.atmosres.2016. 07.014.

Giles, B.D., Flocas, A.A., 1990. Diurnal rainfall variations in Thessaloniki, Greece. Theor. Appl. Climatol. 41, 221–225.

Hirose, H., 1994. Parameter estimation in the extreme value distributions using the continuation method. Trans. Inf. Proces. Soc. Jpn. 35 (9), 1674–1681.

Huschke, R.E., 1959. Glossary of Meteorology. American Meteor Society, Boston, Mass (464pp).

IPCC, 2007. Climate change 2007: the physical science basis. In: Solomon, S., Qin, D., Manning, M., Chen, Z., Marquis, M., Averyt, K.B., Tignor, M., Miller, H.L. (Eds.), Contribution of Working Group I to the Fourth Assessment. Report of the Intergovernmental Panel on Climate Change. Cambridge University Press, Cambridge, United Kingdom/New York, NY, USA (996pp).

Kanae, S., Oki, T., Kashida, A., 2004. Changes in hourly heavy precipitation at Tokyo from 1890 to 1999. J. Meteorol. Soc. Jpn. 82, 241–247.

Karagiannidis, A.F., Karacostas, T., Maheras, P., Makrogiannis, T., 2012. Climatological aspects of extreme precipitation in Europe, related to mid-latitude cyclonic systems. Theor. Appl. Climatol. 107, 165–174.

Koutsoyiannis, D., 2004. Statistics of extremes and estimation of extreme rainfall: II. Empirical investigation of long rainfall records. Hydrol. Sci. J. 499 (4), 591–610.

Lenderink, G., Mok, H.Y., Lee, T.C., Oldenborgh, G.J., 2011. Scaling and trends of hourly precipitation extremes in two different climate zones—Hong Kong and the Netherlands. Hydrol. Earth Syst. Sci. J. 15 (9), 3033–3041.

Matsumoto, M., Nishimura, T., 1998. Mersenne twister: a 623-dimensionally equidistributed uniform pseudo-random number generator. ACM Trans. Model. Comput. Simul. 8, 3–30.

Mayooran, T., Laheetharan, A., 2014. The statistical distribution of annual maximum rainfall in Colombo District. Sri Lankan J. Appl. Stat. 15–2.

Müller, M., Kašpar, M., Řezáčová, D., Sokol, Z., 2009. Extremeness of meteorological variables as an indicator of extreme precipitation events. Atmos. Res. 92, 308–317. http://dx.doi.org/10.1016/j.atmosres.2009.01.010.

Nadarajah, S., Withers, C.S., 2001. Evidence of trend in return levels for daily rainfall in New Zealand. J. Hydrol. N. Z. 39, 155–166.

Pakalidou, N., Karacosta, P., 2016. Statistical analysis of a 124-year period of precipitation data in Thessaloniki. 537–543. In: Karacostas, T.S., Bais, A.F., Nastos, P.T. (Eds.), Perspectives on Atmospheric Sciences. Springer Atmospheric Sciences Vol. I Springer-Verlag Berlin Heidelberg. http://dx.doi.org/10.1007/978-3-319-35095-0. (1259pp. ISBN 978-3-319-35094-3, ISBN 978-3-319-35095-0 (eBook)).

RamachandraRao, A., Hamed, K.H., 2000. Flood Frequency Analysis. CRC Press, Boca Raton, Florida, USA, pp. 6–7.

Reimann, C., Filzmoser, P., Garrett, R.G., 2005. Background and threshold: critical comparison of methods of determination. Sci. Total Environ. 346, 1–16.

Santos, M., Fragoso, M., 2013. Precipitation variability in Northern Portugal: data homogeneity assessment and trends in extreme precipitation indices. Atmos. Res. 131, 34–45.

Sen, R.S., 2008. A spatial analysis of extreme hourly precipitation patterns in India. Int. J. Climatol. 29, 345–355.

Snedecor, G., Cochran, W., 1989. Statistical Methods, Eighth Edition. Iowa State University Press.

Song, X., Song, S., Sun, W., Mu, X., Wang, S., Li, J., Li, Y., 2015. Recent changes in extreme precipitation and drought over the Songhua River Basin, China, during 1960–2013. Atmos. Res. 157, 137–152.

Stathis, D., Mavromatis, T., 2009. Characteristics of precipitation in Thessaloniki area, north Greece. Fresenius Environ. Bull. 18 (7), 1–6.

Stephens, M.A., 1974. EDF statistics for goodness of fit and some comparisons. J. Am. Stat. Assoc. 69, 730–737.

Trenberth, K.E., 1999. Conceptual framework for changes of extremes of the hydrological cycle with climate change. Clim. Chang. 42, 327–339.

Twardosz, R., 2010. An analysis of diurnal variations of heavy hourly precipitation in Kraków using a classification of circulation types over Poland. Phys. Chem. Earth 35, 456–461.

Wilks, D.S., 2006. Statistical methods in the atmospheric sciences. In: International Geophysics Series, 2nd edn. Vol 91 Academic Press (627 pp).

Winkler, J.A., 1992. Regional patterns of the diurnal properties of heavy hourly precipitation. Prof. Geogr. 44, 127–146.

Xu, X., Du, Y., Tang, J., Wang, Y., 2011. Variations of temperature and precipitation extremes in recent two decades over China. Atmos. Res. 101 (1–2), 143–154.

Zalina, M.D., Desa, M.N., Nguyen, V.T.V., Hashim, M.K., 2002. Selecting a probability distribution for extreme rainfall series in Malaysia. Water Sci. Technol. 45, 63–68.